Biochemical Pharmacology 86 (2013) 458–468

Contents lists available at SciVerse ScienceDirect

Biochemical Pharmacology

journal homepage: www.elsevier.com/locate/biochempharm

Utilization of 6-(methylsulfinyl)hexyl isothiocyanate for sensitization of tumor cells to antitumor agents in combination therapies

Hideaki Yamaguchi [a,*], Yumi Kidachi [b], Katsuyoshi Kamiie [b], Toshiro Noshita [c], Hironori Umetsu [d], Yoko Fuke [e], Kazuo Ryoyama [b]

[a] Department of Pharmacy, Faculty of Pharmacy, Meijo University, 150 Yagotoyama, Tenpaku, Nagoya 468-8503, Japan
[b] Department of Pharmacy, Faculty of Pharmaceutical Sciences, Aomori University, 2-3-1 Kobata, Aomori 030-0943, Japan
[c] Department of Life Sciences, Faculty of Life and Environmental Sciences, Prefectural University of Hiroshima, 562 Nanatsuka, Shobara 727-0023, Japan
[d] Laboratory of Food Chemistry, Department of Life Sciences, Junior College, Gifu Shotoku Gakuen University, 1-38 Nakauzura, Gifu 055-8288, Japan
[e] Department of Health Promotion Sciences, Graduate School of Human Health Sciences, Tokyo Metropolitan University, 1-1 Minami-Osawa, Hachioji 192-0397, Japan

ARTICLE INFO

Article history:
Received 24 April 2013
Accepted 12 June 2013
Available online 19 June 2013

Keywords:
6-(Methylsulfinyl)hexyl isothiocyanate (6-MITC)
Glutathione (GSH)
Glutamate cysteine ligase (GCL)
Glutamate cysteine ligase catalytic subunit (GCLC)

ABSTRACT

In the present study, we performed *in silico* and *in vitro* analyses to evaluate the chemosensitizing effects of 6-(methylsulfinyl)hexyl isothiocyanate (6-MITC) on tumor cells. Our *in silico* analyses of the ligand–receptor interactions between 6-MITC and the glutamate cysteine ligase (GCL) catalytic subunit (GCLC) revealed that 6-MITC possibly inhibited GCL enzyme activity, and that Cys-249 and Gln-251 were important residues for stable binding of ligands to GCLC. It was further found that 6-MITC interfered with the hydrogen bonds of the cysteinyl and glutamyl moieties of GSH with Cys-249 and Gln-251, respectively, and possibly overrode the feedback inhibition of GCL enzyme activity by GSH. To the best of our knowledge, this is the first *in silico* analysis to suggest an overriding effect of 6-MITC on GSH-induced feedback inhibition of GCL. In our *in vitro* analyses, combined treatment with 6-MITC and L-buthionine-*S*,*R*-sulfoximine (BSO) depleted GSH within 4 h in tumorigenic human c-Ha-*ras* and mouse c-*myc*-cotransfected highly metastatic serum-free mouse embryo-1 (*r*/*m* HM-SFME-1) cells, but did not deplete GSH in normal SFME cells. Furthermore, exposure to 6-MITC plus BSO for 4 h, followed by glycyrrhetinic acid (GA) treatment for 3 h, eradicated the tumor cells with minimal damage to the normal cells. The present findings suggest that 6-MITC in combination therapies could be used to sensitize tumor cells to antitumor agents, thereby leading to their eradication.

1. Introduction

Isothiocyanates (ITCs) have long been known to be abundant in a variety of vegetables, particularly some species of crucifers [1,2]. There is growing interest in ITCs because of findings that they offer chemoprotection against tumor formation in a variety of animal models [3–8]. The antitumor activities of ITCs largely involve modulation of carcinogen metabolism through inhibition of phase 1 enzymes and/or induction of phase 2 enzymes, such as GSH S-transferase and quinone reductase [9–15]. 6-(Methylsulfinyl)hexyl isothiocyanate (6-MITC) is found in wasabi (*Wasabia japonica*), a Japanese indigenous herb, and this compound with its antitumor properties has been attracting great attention as a possible new candidate for controlling tumor cell progression and metastasis [16,17]. 6-MITC showed antitumor activity in a human cancer cell (HCC) panel, and specific suppression was found for the growth and survival of breast cancer and melanoma cell lines. Based on the HCC database, a computerized analysis, "COMPARE", was applied, which suggested that the suppression mechanism of 6-MITC was unique, involved multiple pathways, and might be different from those of other known chemicals [16]. 6-MITC also exhibited antitumor activity in a mouse model of pulmonary metastasis. Administration of 6-MITC significantly reduced the number of

Abbreviations: ABC, ATP-binding cassette; ANOVA, analysis of variance; AP-1, activating protein 1; ASE-Dock, alpha sphere and excluded volume-based ligand-protein docking; BSO, L-buthionine-*S*,*R*-sulfoximine; CORT, corticosterone; GA, glycyrrhetinic acid; GCL, glutamate cysteine ligase; GCLC, glutamate cysteine ligase catalytic subunit; GCLM, glutamate cysteine ligase modifier subunit; HCC, human cancer cell; ITC, isothiocyanate; JNK, Jun N-terminal kinase; LBS, ligand-binding site; LTA4, leukotriene A4; MOE, molecular operating environment; MRP1, multidrug resistance protein 1; NAC, *N*-acetyl-L-cysteine; NF-κB, nuclear factor κB; *r*/*m* HM-SFME-1, human c-Ha-*ras* and mouse c-*myc*-cotransfected highly metastatic serum-free mouse embryo-1; ROS, reactive oxygen species; SFME, serum-free mouse embryo; 4-HNE, 4-hydroxynonenal; 6-MITC, 6-(methylsulfinyl)hexyl isothiocyanate; 11βHSD2, 11β-hydroxysteroid dehydrogenase type 2; 11DHC, 11-dehydrocorticosterone.

* Corresponding author. Tel.: +81 52 839 2721; fax: +81 52 834 8090.
E-mail address: hyamagu@meijo-u.ac.jp (H. Yamaguchi).

0006-2952/$ – see front matter © 2013 Elsevier Inc. All rights reserved.
http://dx.doi.org/10.1016/j.bcp.2013.06.008

metastasized melanoma cells in the lungs and inhibited foci formation, when murine B16-BL6 melanoma cells were injected subcutaneously or intravenously into C57BL/6J mice [17]. Furthermore, in our previous study, 6-MITC demonstrated significant growth inhibitory activity toward a macrophage-like tumor cell line [18]. Taken together, these reports suggest that 6-MITC can be used as a potential therapeutic option for controlling cancer.

GSH is an intracellular tripeptide antioxidant and the major low-molecular-weight cellular thiol. Reduced GSH is present in most cell types at millimolar levels, whereas the oxidized form, GSH disulfide, is less abundant [19]. GSH plays roles in many cellular functions, such as amino acid transport, maintenance of reduced protein thiols and cellular redox potential, detoxification of hydrogen peroxide and lipid peroxides, and non-enzymatic scavenging of free radicals [19,20]. It also acts as a source of cysteine for protein formation, reduces disulfides to sulfides, and is involved in the formation of deoxyribonucleotides from ribonucleotides [20,21]. In addition, GSH protects against apoptotic cell death following exposure to toxins of both endogenous and exogenous origin, antineoplastic agents, radiation, and receptor-based death signals [22–25]. GSH is synthesized through the actions of two enzymes, glutamate cysteine ligase (GCL) and GSH synthetase. GCL is the enzyme that catalyzes the initial and rate-limiting step of GSH biosynthesis [26,27]. For synthesis of the GSH tripeptide, the ATP-dependent mechanism proceeds *via* a γ-glutamylphosphate intermediate, with a subsequent nucleophilic attack by the α-amino group of L-cysteine to form the dipeptide γ-glutamylcysteine. GSH synthetase then couples the cysteine carboxyl group of γ-glutamylcysteine to L-glycine to generate reduced GSH, the abundant cellular reducing agent [26–29]. GCL is a heterodimer composed of a heavy catalytic subunit (73 kDa; GCLC) and a light modifier subunit (31 kDa; GCLM) that associate with each other through disulfide bonds to form the holoenzyme. GCLC exhibits all of the catalytic activity of the enzyme and is also the site of feedback inhibition by GSH. It is encoded by a gene located on chromosome 6p12. GCLM is encoded by a gene on chromosome 1p21.6, and increases the affinity of GCLC for its ligands (substrates), glutamate and cysteine [30–32].

Our previous study revealed that downregulation of GSH was an important factor for selective toxicity toward CNS-derived tumor cells [33], suggesting that targeting of the key enzyme for GSH homeostasis, namely GCL, with highly selective inhibitors could be used to control the development and progression of cancer. In fact, upregulation of GCLC mRNA expression and GCL activity has frequently been observed in cells derived from human tumors that are resistant to chemotherapeutic agents [34–36], and elevated GSH levels have been implicated in cellular resistance to irradiation and antitumor drugs, such as alkylating agents, platinum compounds, topoisomerase inhibitors, and taxanes [37–40]. It has been reported that drug resistance in tumors can be overcome by administration of the GCL inhibitor L-buthionine-*S*,*R*-sulfoximine (BSO) [41–43], which subsequently downregulates GSH and sensitizes the tumor cells to radiation treatment and chemotherapy. However, owing to difficulties associated with the production of BSO and its analogs, in addition to their limited potency for GSH depletion [27,41,44,45], it is desirable to develop novel antitumor compounds or strategies that can effectively deplete GSH.

In the present study, we performed the first *in silico* structural analyses of the ligand–receptor interactions between 6-MITC and GCLC, as the catalytic subunit of GCL and crucial enzyme for GSH biosynthesis, to evaluate the potency of 6-MITC as a GSH downregulator for antitumor therapies. Ligand fitting of 6-MITC to GCLC was analyzed by a molecular modeling method to predict its inhibitory effects toward the enzyme. Ligand–receptor interaction plots for 6-MITC-GCLC complexes were created to investigate the arrangement of the key intermolecular interactions, and the ligand–residue interaction energies were calculated. *In vitro* analyses were also conducted to confirm the findings of the *in silico* analyses. Normal cells and tumor cells were treated with 6-MITC and BSO, and analyzed for their cellular GSH contents to examine whether GSH can be downregulated and eventually depleted by these compounds. The effects of 6-MITC on the GCL enzyme activity were also investigated. Furthermore, after exposure to 6-MITC plus BSO, which was the most potent treatment for GSH downregulation, the cells were treated with an antitumor compound, glycyrrhetinic acid (GA), and analyzed for their cell growth to explore 6-MITC-utilizing antitumor strategies that can induce strong cell toxicity toward tumor cells without affecting normal cells.

2. Materials and methods

2.1. Materials

6-MITC was obtained from Shiratori Pharmaceuticals (Chiba, Japan). BSO, *N*-acetyl-L-cysteine (NAC), and GA were purchased from Sigma–Aldrich Chemical Co. (St. Louis, MO). GSH was from Wako Pure Chemical Industries Ltd. (Osaka, Japan).

2.2. In silico *ligand–receptor interactions between 6-MITC and GCLC*

Homology modeling of GCLC and its binding site selection and exploration were carried out as previously reported [46,47]. Briefly, yeast GCLC (PDB code: 3LVV) [48] was selected as a template for the structural modeling of human GCLC (NCBI reference sequence: NP_001489.1) because of its good crystal structure resolution (2.2 Å) and because its information was the latest (from 2010) among the reported GCLC models. For construction of the GCLC model, 100 independent models of the target protein were built using a Boltzmann-weighted randomized modeling procedure in the Molecular Operating Environment 2010.10 (MOE; Chemical Computing Group Inc., Montreal, Canada) that was adapted from reports by Levitt [49] and Fechteler et al. [50]. The intermediate models were evaluated by a residue packing quality function, which was sensitive to the degrees to which non-polar side-chain groups were buried and hydrogen bonding opportunities were satisfied. The GCLC model with the best packing quality function and full energy minimization was selected for further analyses. Hydrophobic or hydrophilic alpha spheres, which were created by the Site Finder module of the MOE, were used to define potential ligand-binding sites (LBSs).

Analyses of the ligand–receptor interactions between 6-MITC and the GCLC model were performed with the alpha sphere and excluded volume-based ligand–protein docking (ASE-Dock) module of the MOE [51]. In the ASE-Dock module, ligand atoms had alpha spheres within 1 Å. Based on this property, concave models were created and ligand atoms from a large number of conformations generated by superimposition with these points were evaluated and scored by the maximum overlap with the alpha spheres and minimum overlap with the receptor atoms. The ligand docking score was then obtained [52]. The scoring function used by the ASE-Dock module was based on the ligand–receptor interaction energies and the scores were expressed as U_{total} values. The ligand conformations were subjected to energy minimization using the MMF94S force field [53], and 500 conformations were generated using the default systematic search parameters. Five thousand poses per conformation were randomly placed onto the alpha spheres located within the LBS in GCLC. From the resulting 500,000 poses, the 200 poses with the lowest U_{total} values were selected for further optimization with the MMF94S force field.

During the refinement step, the ligands were free to move within the binding pocket.

2.3. Cell lines and cell culture

Serum-free mouse embryo (SFME) cells were a gift from Dr. S. Shirahata (Kyushu University, Fukuoka, Japan). Human c-Ha-*ras* and mouse c-*myc*-cotransfected highly metastatic SFME-1 (*r*/*m* HM-SFME-1) [54] and murine macrophage-like J774.1 [18] cells were taken from our cell stocks. Lung squamous carcinoma RERF-LC-AI cells were obtained from RIKEN BioResource Center (Tsukuba, Japan). The basal nutrient medium for SFME and *r*/*m* HM-SFME-1 cells was a 1:1 mixture of DMEM and nutrient mixture F-12 Ham, supplemented with sodium bicarbonate, sodium selenite, gentamicin sulfate, insulin, transferrin, and EGF (Sigma–Aldrich Chemical Co.). RERF-LC-AI cells were cultured in EME medium supplemented with L-glutamine, sodium bicarbonate, penicillin, streptomycin, and FBS (Sigma–Aldrich Chemical Co.). J774.1 cells were grown in RPMI1640 medium supplemented with gentamicin sulfate and FBS (Sigma–Aldrich Chemical Co.). All the cells were maintained in a humidified atmosphere containing 20% O_2 and 5% CO_2 at 37 °C.

2.4. Measurement of cell viability

Cells plated at 1×10^4 cells/well in 96-well microplates were treated with the test compounds at half-confluency. After culture for 1–6 h, the cell numbers were determined by the MTT assay [55].

2.5. Measurement of GSH levels

Cellular GSH levels were determined as previously reported [47]. Briefly, cells were treated with the test compounds at half-confluency and incubated for 4–24 h. GSH production was analyzed using a Glutathione Assay Kit (BioVision, Mountain View, CA). In this kit, GSH reacted with *o*-phthalaldehyde and the generated fluorescence was measured with 340 nm excitation and 420 nm emission. Each value was expressed as picomol/10^3 cells.

2.6. Western blotting analysis

Proteins were extracted with PBS containing 1 mM PMSF, 1 mM EDTA, 2 mM 2-mercaptoethanol, and 1% Triton X-100 (Sigma–Aldrich Chemical Co.) at 4 °C for 3.5 h. For Western blotting analysis, aliquots of proteins were separated by SDS-PAGE, transferred to a nitrocellulose membrane, and probed with a primary antibody followed by a secondary antibody. The primary antibodies used were mouse monoclonal anti-GAPDH (Santa Cruz Biotechnology, Santa Cruz, CA), rabbit polyclonal anti-GCLC (Santa Cruz Biotechnology), and rabbit polyclonal anti-GCLM (Santa Cruz Biotechnology). The secondary antibodies used were alkaline phosphatase-conjugated anti-mouse and anti-rabbit IgG_1 (Chemicon International, Temecula, CA). Visualization of the antigen–antibody complexes was performed with 33 μl of 5-bromo-4-chloro-3-indolyl phosphate, 66 μl of nitroblue tetrazolium, and 40 μl of 1 M $MgCl_2$ in 10 ml of 0.1 M Tris-HCl buffer (pH 9.5). Images of the positive bands were obtained by scanning and the densities were determined using an LAS-3000 image analyzer (Fuji Film, Tokyo, Japan).

2.7. Measurement of GCL enzyme activity

GCL enzyme activity was assessed by the methods of Huang et al. [56] with some minor modifications, by monitoring the

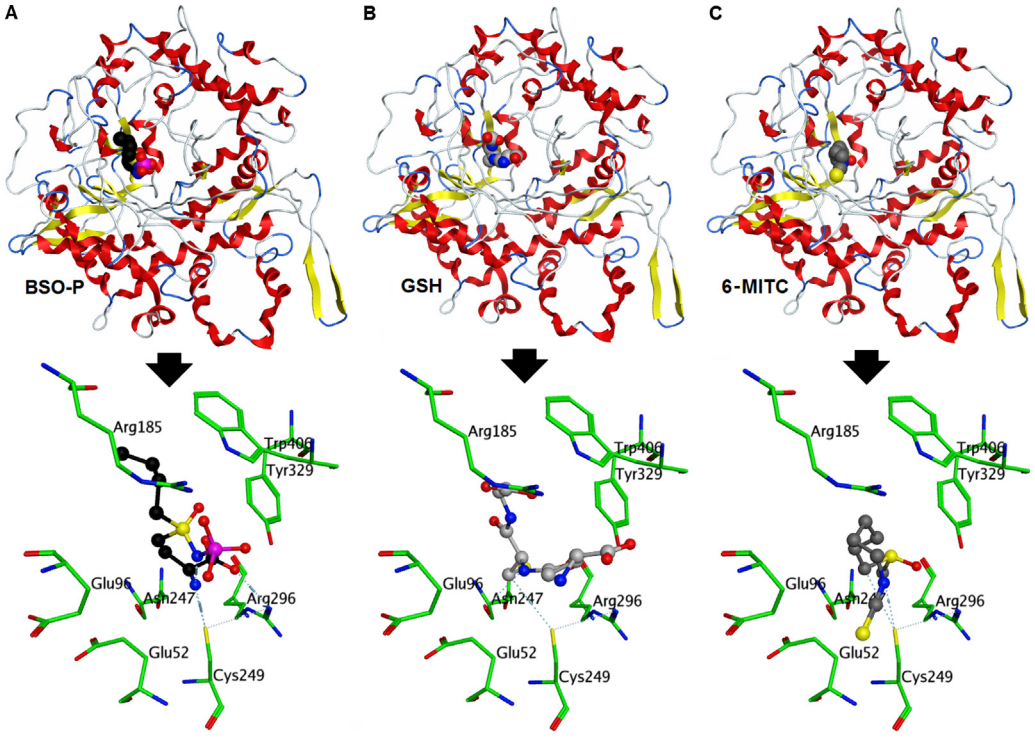

Fig. 1. ASE-Dock findings between the test compounds and the GCLC model. The ASE-Dock module reveals that BSO-P (A, upper panel), GSH (B, upper panel), and 6-MITC (C, upper panel) can bind to the LBS in the GCLC model. The ligand docking scores for BSO-P, GSH, and 6-MITC are −246.5, −147.8, and −31.3, respectively. Black: carbon for BSO-P; blue: nitrogen; dark gray: carbon for 6-MITC; light gray: carbon for GSH; purple: phosphorus; red: oxygen; and yellow: sulfur. The eight key catalytic residues for substrate recognition in GCLC have been identified [48], and our results reveal that BSO-P (A, lower panel), GSH (B, lower panel), and 6-MITC (C, lower panel) form hydrogen bonds with Cys-249. Black: carbon for BSO-P; blue: nitrogen; dark gray: carbon for 6-MITC; green: carbon for residues; light gray: carbon for GSH; purple: phosphorus; red: oxygen; and yellow: sulfur. (For interpretation of the references to color in this figure legend, the reader is referred to the web version of the article.)

decreasing absorbance of NADH at 340 nm. The reaction mixture contained 5 mM L-glutamate, 5 mM L-α-aminobutyrate (cysteine substitute), 10 mM $MgCl_2$, 5 mM ATP, 2 mM phosphoenolpyruvate, 150 mM KCl, 0.2 mM NADH, 5 U of pyruvate kinase (Sigma–Aldrich Chemical Co.), and 10 U of lactate dehydrogenase (Sigma–Aldrich Chemical Co.) in 100 mM Tris–HC1 (pH 8.2), and also contained 100 μM BSO, 5 mM GSH (0–2 mM for determination of K_m values), 5 μM 6-MITC (0–10 mM for determination of K_m values), or combinations of these compounds as GCL inhibitors. The preparation of GCL for the reaction mixture was performed by the methods of Biterova and Barycki [57], and the samples were incubated at 37 °C for 30 min.

2.8. Statistical analysis

Experiments were performed in triplicate and repeated at least three times. The values are given as means ± SD. Ordinary or repeated-measures analysis of variance (ANOVA) followed by the Tukey–Kramer multiple comparison test was used to evaluate the statistical significance of differences between groups.

3. Results

3.1. Ligand–receptor interactions between 6-MITC and GCLC

The ASE-Dock module revealed that 6-MITC could bind to the LBS in the GCLC model in addition to phosphorylated BSO (BSO-P; the transition state analog) and GSH as GCL inhibitors (Fig. 1A–C, upper panels). The ligand docking scores for BSO-P, GSH, and 6-MITC were −246.5, −147.8, and −31.3 kcal/mol, respectively. The eight key catalytic residues for substrate recognition in GCLC have been identified [48], and our results revealed that all of the tested ligands, including 6-MITC, formed hydrogen bonds with Cys-249 (Fig. 1A–C, lower panels). Furthermore, the ligand–residue interaction energies were calculated by the method of Labute [58], which assigns energy terms in kcal/mol for each residue. Generally, a negative value indicated that the residue attracted the ligand, while a positive value indicated that the residue repelled the ligand. Arg-185, Arg-296, and Arg-427 in GCLC showed higher negative values, while Glu-50 had a higher positive value, for BSO-P-GCLC interaction energies (Fig. 2A, upper panel). Glu-50, Arg-185, Lys-412, and Arg-427 exhibited higher negative values for

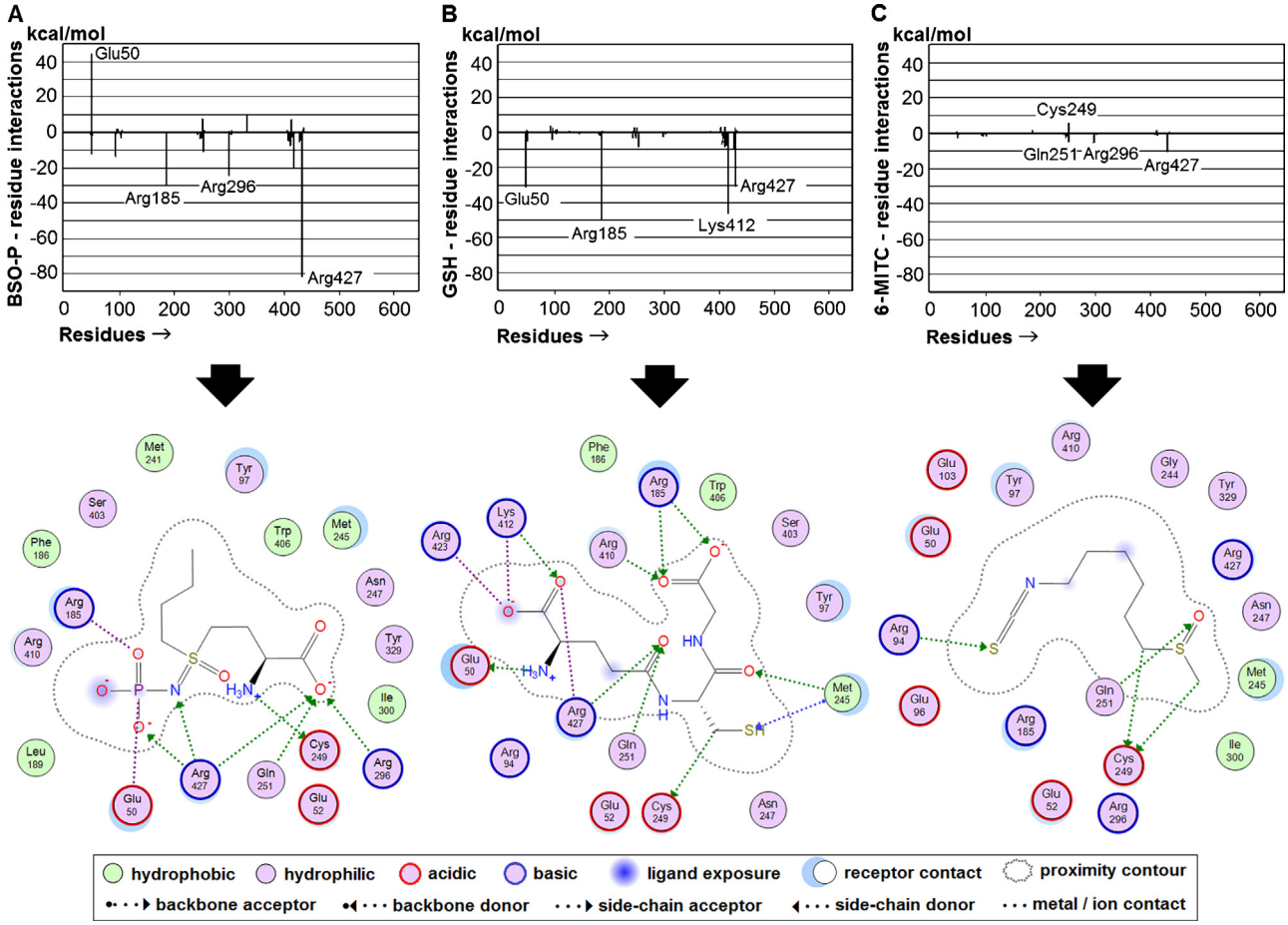

Fig. 2. Ligand–residue interaction energies and ligand–receptor interaction plots for the ligand–GCLC complexes. (A, upper panel) Arg-185, Arg-296, and Arg-427 in GCLC show higher negative values, while Glu-50 has a higher positive value for BSO-P-GCLC interaction energies. (B, upper panel) Glu-50, Arg-185, Lys-412, and Arg-427 exhibit higher negative values for GSH-GCLC. (C, upper panel) Although 6-MITC-GCLC shows smaller energy values, Cys-249, Gln-251, Arg-296, and Arg-427 are identified as interacting residues. (A, lower panel) Hydrogen bonds are found between BSO-P and Cys-249, Gln-251, Arg-296, and Arg-427. Ionic bonds are also found between BSO-P and Glu-50 and Arg-185. Although the hydrophobic and hydrophilic interactions are sporadic, BSO-P shows some hydrophobic interactions with the residues. (B, lower panel) Glu-50, Arg-185, Met-245, Cys-249, Gln-251, Arg-410, Lys-412, and Arg-427 form hydrogen bonds with GSH. Ionic bonds are also found between GSH and Lys-412, Arg-423, and Arg-427. (C, lower panel) 6-MITC exhibits hydrogen bonds with Arg-94, Cys-249, and Gln-251. The 2D diagrams also reveal the reported hydrophobic pocket [57] lined by Tyr-97, Phe-186, Leu-189, Met-241, Met-245, and Trp-406 in the BSO-P-GCLC complex (A, lower panel). However, only four and two of these six residues are identified as interacting residues in the GSH-GCLC (B, lower panel) and 6-MITC-GCLC (C, lower panel) complexes, respectively.

GSH-GCLC (Fig. 2B, upper panel). Although 6-MITC-GCLC showed smaller energy values, Cys-249, Gln-251, Arg-296, and Arg-427 were identified as interacting residues (Fig. 2C, upper panel). Furthermore, to create ligand–receptor interaction plots for each ligand–GCLC complex, the ligand interactions module of the MOE was used, which provided a clearer arrangement of the putative key intermolecular interactions that aid in the interpretation of the 3D juxtaposition of the ligands and the LBS in GCLC (Fig. 2A–C, lower panels). Our results revealed the presence of hydrogen bonds between BSO-P and Cys-249, Gln-251, Arg-296, and Arg-427. Ionic bonds were also found between BSO-P and Glu-50 and Arg-185. Although the hydrophobic and hydrophilic interactions were sporadic, BSO-P showed some hydrophobic interactions with the residues (Fig. 2A, lower panel). GSH formed hydrogen bonds with Glu-50, Arg-185, Met-245, Cys-249, Gln-251, Arg-410, Lys-412, and Arg-427. Ionic bonds were also found between GSH and Lys-412, Arg-423, and Arg-427 (Fig. 2B, lower panel). 6-MITC exhibited hydrogen bonds with Arg-94, Cys-249, and Gln-251 (Fig. 2C, lower panel). The 2D diagrams further revealed the reported hydrophobic pocket [57] lined by Tyr-97, Phe-186, Leu-189, Met-241, Met-245, and Trp-406 in the BSO-P-GCLC complex (Fig. 2A, lower panel). However, only four and two of these six residues were identified as interacting residues in the GSH-GCLC (Fig. 2B, lower panel) and 6-MITC-GCLC (Fig. 2C, lower panel) complexes, respectively.

3.2. Effects of 6-MITC on cell growth and cellular GSH in normal cells and tumor cells

The normal SFME cells and tumor cells (J774.1, *r*/*m* HM-SFME-1, and RERF-LC-AI) were treated with 100 μM BSO and/or 5 μM 6-MITC for 4 h and the effects on their cell growth and cellular GSH were examined. As shown in Fig. 3A, none of the treatments damaged the normal cells or tumor cells. However, the cellular GSH in all cell types was significantly decreased by all treatments (Fig. 3B). Although there was a trend that 6-MITC might be more effective than BSO for GSH downregulation, a significant difference was not found. The effects of BSO plus 6-MITC were prominent, and this treatment downregulated cellular GSH by 67%, 85%, and 93% in J774.1, RERF-LC-AI, and *r*/*m* HM-SFME-1 cells, respectively. The cellular GSH in normal SFME cells was decreased by 80% by BSO plus 6-MITC.

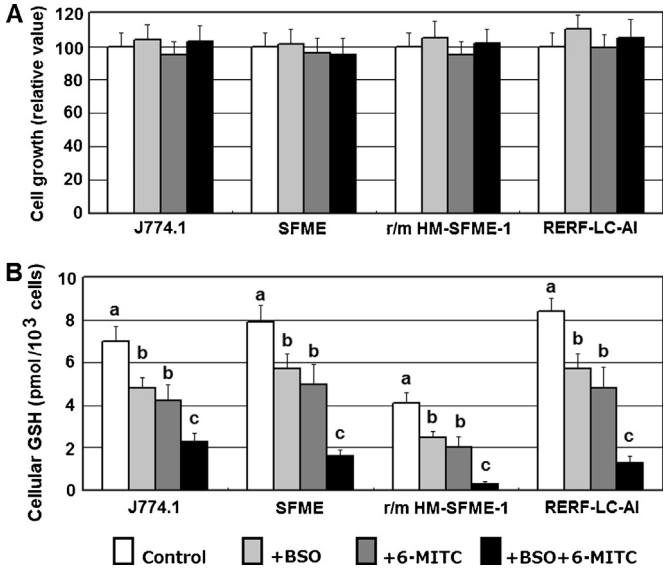

Fig. 3. Effects of 4 h exposure to the test compounds on cell growth and cellular GSH in normal cells and tumor cells. Normal SFME cells and tumor cells (J774.1, *r*/*m* HM-SFME-1, and RERF-LC-AI) were treated with 100 μM BSO and/or 5 μM 6-MITC for 4 h and the effects on cell growth and cellular GSH were examined. (A) None of the treatments damage the normal cells or tumor cells. (B) Cellular GSH in all cell types is significantly decreased by all treatments. The effects of BSO plus 6-MITC are prominent, and this treatment downregulates cellular GSH by 67%, 85%, and 93% in J774.1, RERF-LC-AI, and *r*/*m* HM-SFME-1 cells, respectively. The cellular GSH in normal SFME cells is decreased by 80% by treatment with BSO plus 6-MITC. The data represent means ± SD of three experiments. Different letters for the treatments indicate significant differences by the Tukey–Kramer test ($P < 0.05$).

3.3. Effects of 24 h exposure to BSO plus 6-MITC on cellular GSH in normal cells and tumor cells

Thus far, we had analyzed the 4 h effects of the test compounds on cellular GSH, and found that treatment with BSO plus 6-MITC was the most effective (Fig. 3B). However, the treatment could not achieve total depletion of GSH in tumor cells. Furthermore, it is important for an antitumor drug treatment that the GSH decrease in tumor cells is maximal, while that in normal cells is minimal. Therefore, we extended the treatment time to 24 h to determine whether cellular GSH in tumor cells could be depleted, with a minimal effect on cellular GSH in normal cells, during a long period of exposure to the test compounds. As shown in Fig. 4A–D, depletion of GSH was achieved by 12 h in all cell types after treatment with BSO plus 6-MITC. This treatment was very effective on *r*/*m* HM-SFME-1 cells, as the tumor cell line of normal SFME cells, in which cellular GSH was almost completely depleted by 4 h (Fig. 4C), while cellular GSH depletion was achieved by 12 h in SFME cells (Fig. 4B), 12 h in J774.1 cells (Fig. 4A), and 8 h in RERF-LC-AI cells (Fig. 4D). Interestingly, with 6-MITC treatment, the cellular GSH in all cell types started to increase at 4 h, continued to increase until 12 h, even exceeding the control values, and then gradually decreased (Fig. 4A–D). Therefore, *r*/*m* HM-SFME-1 cells (the cell line most affected by BSO plus 6-MITC treatment) were treated with 6-MITC for 8, 16, and 24 h, and its effects on GCLC and GCLM expression were analyzed to elucidate the increasing effects of 6-MITC on cellular GSH. As shown in Fig. 4E, the GCLC and GCLM expression levels were both increased in a time-dependent manner by 16 h, and then slightly decreased in the 6-MITC-treated tumor cells.

3.4. Structural analysis of the 6-MITC-GCLC model in GSH feedback inhibition override

It has been reported that GSH induces feedback inhibition of GCL and decreases cellular GSH [32]. We surmised that the GSH upregulation by 6-MITC (Fig. 4A–D) could be attributed to 6-MITC interference with the binding of GSH to GCLC. Thus, we conducted further *in silico* structural analyses of the 6-MITC-GCLC model to ascertain whether 6-MITC could interfere with GSH binding to GCLC. The ASE-Dock module revealed that GSH and 6-MITC had similar binding orientations in the GCLC model (Fig. 5A and B) and that 6-MITC could interfere with the hydrogen bond of the cysteinyl moiety of GSH (Fig. 5C). This interference was also found in the 2D diagrams, in which 6-MITC formed hydrogen bonds with Cys-249 and Gln-251 in the LBS in GCLC (Fig. 2C, lower panel), competing with the cysteinyl and glutamyl moieties of GSH that also interacted with Cys-249 and Gln-251, respectively (Fig. 2B, lower panel). Furthermore, a two-ligand docking analysis was performed with the ASE-Dock module, and showed that GSH was unable to enter the LBS in GCLC when 6-MITC was bound to the LBS (Fig. 5D). This observation indicates that 6-MITC can interfere with the feedback inhibition of GCL by GSH. In contrast, γ-glutamylcysteine, the final product of GCLC catalysis, was able to enter the LBS in GCLC in the presence of 6-MITC (Fig. 5E and F), suggesting that although 6-MITC binds to the LBS in GCLC, it may not totally inhibit the enzyme activity of GCL, but only mildly inhibit or

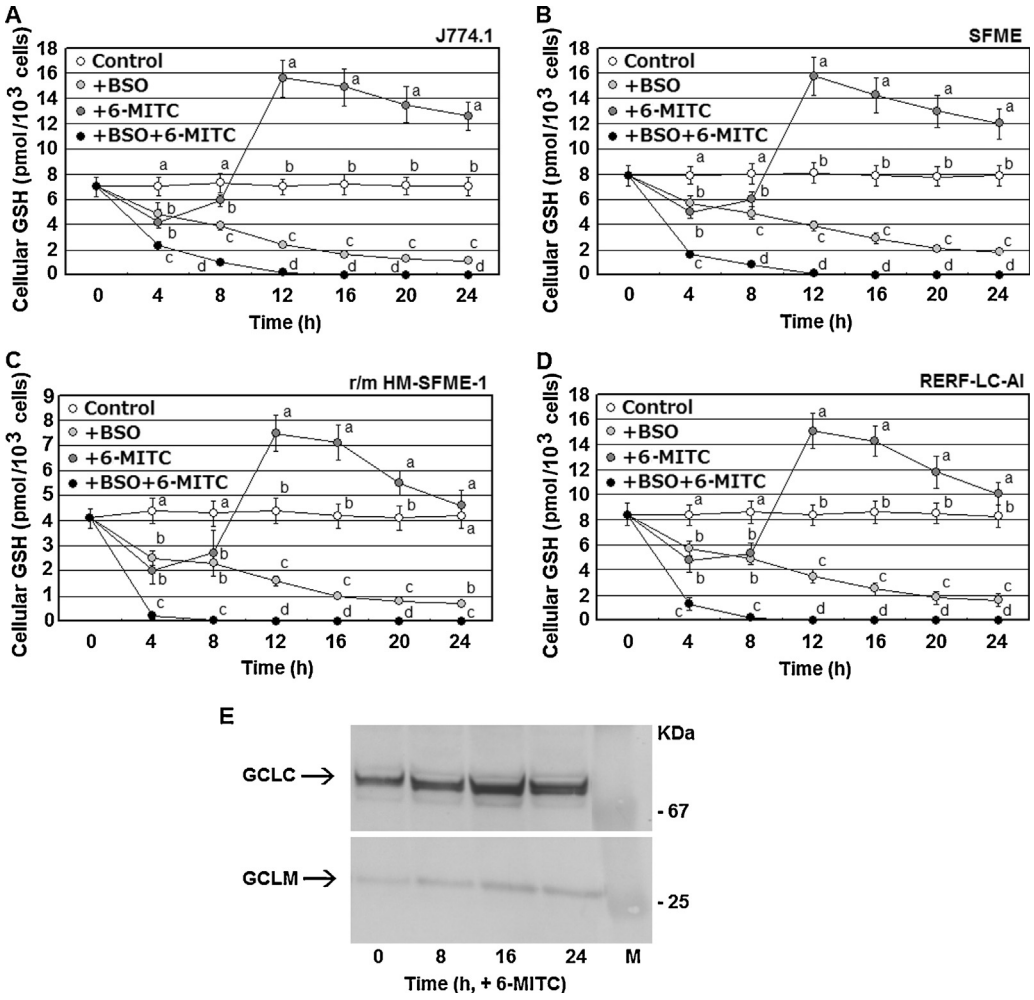

Fig. 4. Effects of 24 h exposure to the test compounds on cellular GSH in normal and tumor cells. Normal SFME cells and tumor cells (J774.1, *r*/*m* HM-SFME-1, and RERF-LC-AI) were treated with 100 μM BSO and/or 5 μM 6-MITC for 24 h to determine whether cellular GSH in tumor cells can be depleted, with a minimal effect on GSH in normal cells, during a long period of exposure to the test compounds. (A–D) Depletion of GSH is achieved in 12 h in J774.1 (A), SFME (B), *r*/*m* HM-SFME-1 (C), and RERF-LC-AI (D) cells by treatment with BSO plus 6-MITC. The cellular GSH is almost completely depleted by 4 h in *r*/*m* HM-SFME-1 cells (C), while its depletion is achieved by 12 h in SFME cells (B), 12 h in J774.1 cells (A), and 8 h in RERF-LC-AI cells (D). The 6-MITC treatment increases cellular GSH in all cell types from 4 h until 12 h. GSH even exceeds the control values, and then gradually decreases after 12 h (A–D). The data represent means ± SD of three experiments. Different letters for the treatments indicate significant differences by the Tukey–Kramer test ($P < 0.05$). (E) Images of a Western blotting analysis. *r*/*m* HM-SFME-1 cells were treated with 6-MITC for 8, 16, and 24 h, and then analyzed for their GCLC and GCLM expression levels (GAPDH was used as a loading control). The GCLC and GCLM expression levels are both increased in a time-dependent manner by 16 h, and then slightly decrease. M, Size markers.

change the functions of the enzyme. In addition, 6-MITC may even override the feedback inhibition of the enzyme and consequently increase cellular GSH.

3.5. Effects of 6-MITC on GCL enzyme activity

Thus far, the structural analyses of the 6-MITC-GCLC model had revealed that 6-MITC was able to bind to GCLC and mildly inhibit the enzyme activity of GCL (Figs. 1, 2,and 5) and also interfere with the feedback inhibition of GCL by GSH (Fig. 5). To confirm these *in silico* results, *in vitro* inhibition of GCL enzyme activity was assessed by measuring the decrease in NADH in the presence of 100 μM BSO, 5 mM GSH, 5 μM 6-MITC, or combinations of these compounds. Treatment with BSO or BSO plus 6-MITC significantly inhibited the GCL enzyme activity (Fig. 6A). 6-MITC may also possibly inhibit the enzyme activity, but its effect would be very weak. Meanwhile, addition of 6-MITC slightly weakened the inhibitory effects of GSH, indicating that 6-MITC may interfere with GSH and override the feedback inhibition of GCL by GSH. Furthermore, 6-MITC showed a very high K_i value of 87.2 mM for L-glutamate (Fig. 6B). The issue of whether or not 6-MITC binds to or inhibits GCL requires further detailed investigations.

3.6. Effects of an antitumor strategy combining BSO plus 6-MITC and GA

Thus far, the BSO plus 6-MITC exposure appeared to be the most effective treatment for downregulation of cellular GSH (Figs. 3 and 4), suggesting that 6-MITC can be used with BSO in antitumor strategies. These findings prompted us to investigate whether GSH-downregulated tumor-cell toxicity could be induced immediately, possibly within a few hours, by an antitumor agent. To this end, we treated the normal cells and tumor cells with BSO and/or 6-MITC for 4 h to downregulate cellular GSH, and then exposed the cells to 5 μM GA, a potent antitumor compound [33]. As shown in Fig. 7A, all of the tested cells were affected by treatment with BSO and GA, but the differences between the cell types were not very considerable. Exposure of the cells to GA after the 4 h 6-MITC treatment also did not show any great differences between the cell types (Fig. 7B). In contrast, obvious cytotoxicity of GA was

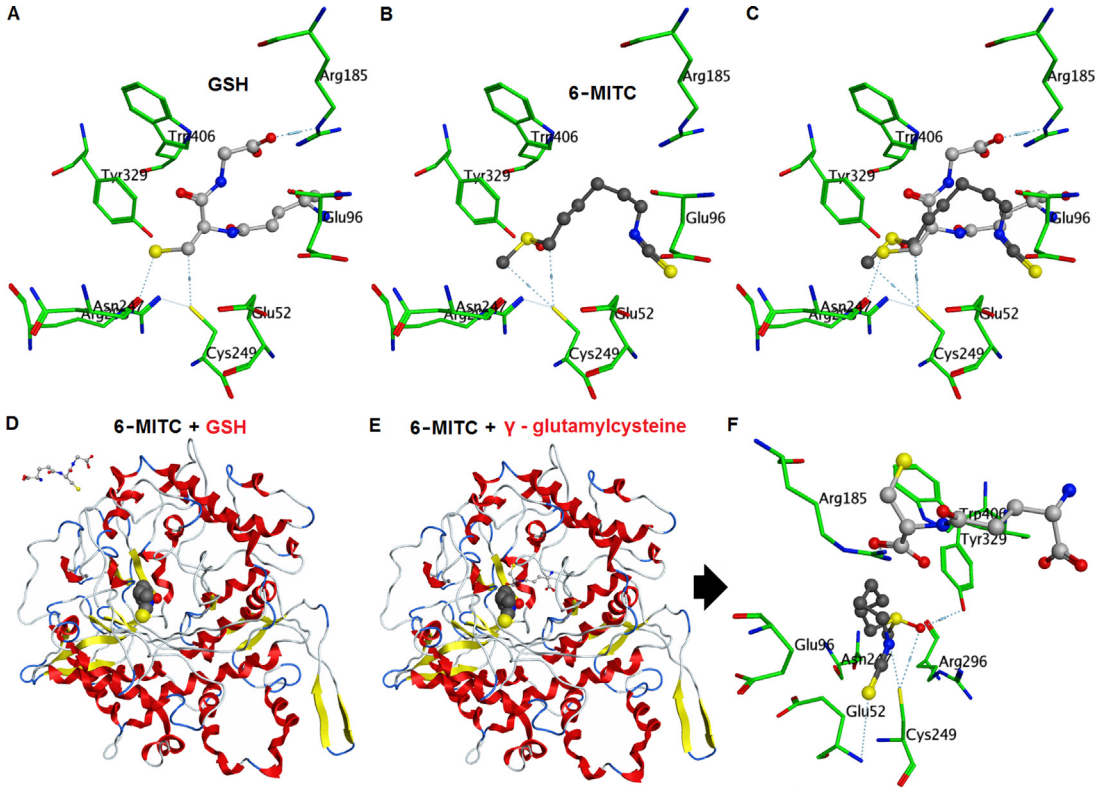

Fig. 5. *In silico* analysis of the 6-MITC-GCLC model for the GSH feedback inhibition override. (A, B) The ASE-Dock module was performed between GSH and GCLC (A) and 6-MITC and GCLC (B). (C) GSH and 6-MITC exhibit similar binding orientations in the GCLC model, and 6-MITC can interfere with the hydrogen bond of the cysteinyl moiety of GSH. (D) A two-ligand docking analysis was also performed with the ASE-Dock module, and showed that GSH is unable to enter the LBS of GCLC when 6-MITC is bound to the LBS, indicating that 6-MITC can interfere with the feedback inhibition of GCL by GSH. (E) In contrast, γ-glutamylcysteine, the final product of the GCLC catalysis, is able to enter the LBS of GCLC in the presence of 6-MITC, suggesting that although 6-MITC binds to the LBS of GCLC, it may not totally inhibit the enzyme activity of GCL, but mildly inhibit or decelerate the function of the enzyme, or even possibly override the feedback inhibition of the enzyme by GSH. (F) LBS of the two-ligand docking model for 6-MITC (ligand), γ-glutamylcysteine (ligand), and GCLC (enzyme). Blue: nitrogen; dark gray: carbon for 6-MITC; green: carbon for residues; light gray: carbon for GSH; red: oxygen; and yellow: sulfur. (For interpretation of the references to color in this figure legend, the reader is referred to the web version of the article.)

observed at an earlier time point (1 h) in the tumor cells (J774.1, RERF-LC-AI, and *r*/*m* HM-SFME-1) compared with the normal SFME cells pretreated with BSO plus 6-MITC (Fig. 7C). In 3 h, GA affected about 30% and 45% of J774.1 and RERF-LC-AI cells, respectively. The effects of GA were more significant on the tumorigenic *r*/*m* HM-SFME-1 cells. GA eradicated the tumor cells within 3 h, while affecting only about 20% of the normal SFME cells in that time. For comparison, it should be noted that single GA treatment required about 96 h to eradicate the tumor cells in a previous study [33]. The effects of GA on the 6-MITC plus BSO-pretreated *r*/*m* HM-SFME-1 cells were attenuated by addition of NAC (Fig. 7D).

4. Discussion

Tumor cells often develop drug resistance through multiple genetic and epigenetic alterations [59,60]. In particular, tumor cells at advanced disease stages exhibit genetic instability and metabolic malfunction, and are often resistant to conventional antitumor drugs [61]. For cancer chemotherapy, sensitization of tumor cells to antitumor drugs is an important issue, and depletion of GSH has been reported to be a useful option [62,63]. In some tumor cell lines, GSH depletion was achieved by BSO and the tumor cells became sensitized to chemotherapeutic agents [64,65]. However, the limited potency of BSO in GSH depletion [27,41,44,45] has necessitated the identification of novel GSH depleters or strategies that can effectively deplete GSH. In the present study, application of 6-MITC, a naturally occurring antitumor compound from *W. japonica*, to GSH depletion for antitumor strategies was explored by *in silico* and *in vitro* analyses.

In silico, the ASE-Dock module revealed that BSO (inhibitor of GCL as the rate-limiting enzyme for GSH production), GSH (feedback inhibitor of GCL), and 6-MITC exhibited similar binding locations in the LBS of the GCLC (catalytic subunit of GCL) model, suggesting that 6-MITC can act as an inhibitor of GCL. The ligand docking scores for the ligand–GCLC docking model revealed that inhibitory effects of the tested compounds on GCL can be presumed in the order of BSO > GSH > 6-MITC. The ligand–residue interaction energies and 2D diagrams also showed that the tested compounds would be more stably located in the LBS of GCLC in the order of BSO > GSH > 6-MITC. Furthermore, the 2D diagrams showed that only four and two of the six residues in the hydrophobic pocket of the BSO-GCLC complex [57] were interacting residues in the GSH-GCLC and 6-MITC-GCLC complexes, respectively, which again indicates that the tested compounds would be more stably located in the LBS of GCLC in the order of BSO > GSH > 6-MITC. Taken together, the results of the *in silico* analyses in the present study suggest that GCL can be inhibited by 6-MITC, although its inhibitory effects are not as strong as those of BSO or GSH. Furthermore, Cys-249 and Gln-251 were the commonly found residues that formed hydrogen bonds with the tested compounds in the present study, and these residues were also identified in other studies [48,57], indicating that they could be important for stable binding of ligands to GCLC. Conservation of side chain functionality in the LBS is supported by mutagenesis

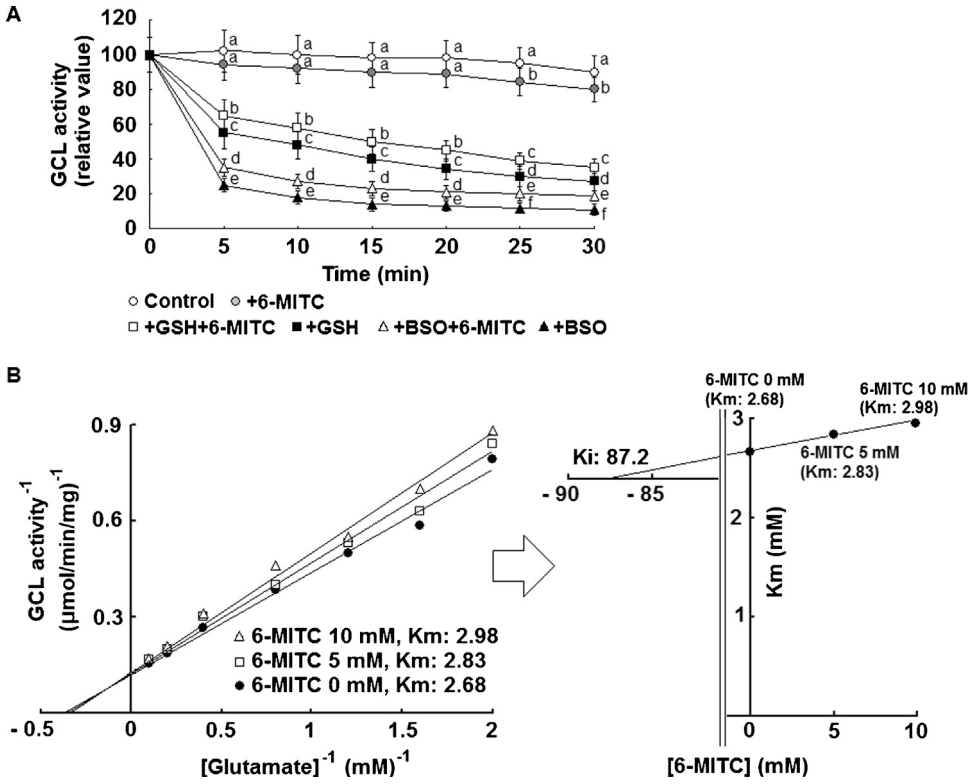

Fig. 6. *In vitro* inhibition of GCL enzyme activity by 6-MITC. (A) Inhibition of GCL enzyme activity was assessed in the presence of 100 μM BSO, 5 mM GSH, 5 μM 6-MITC, or combinations of these compounds. GCL enzyme activity was assessed by the methods of Huang et al. [56] and the preparation of GCL for the reaction mixture was performed by the methods of Biterova and Barycki [57]. 6-MITC inhibits the enzyme activity, but its effect is rather weak. Treatment with BSO or BSO plus 6-MITC significantly inhibits the GCL enzyme activity. Addition of 6-MITC slightly weakens the inhibitory effects of GSH, indicating that 6-MITC can interfere with GSH and override the feedback inhibition of GCL by GSH. The data represent means ± SD of three experiments. Different letters for the treatments indicate significant differences by the Tukey–Kramer test ($P < 0.05$). B) Kinetic analysis for determination of the K_i value of 6-MITC for the GCL enzyme activity. After determination of the K_m values for the GCL enzyme activity with 6-MITC treatment (Lineweaver–Burk plot analysis), the K_i value of 6-MITC for the enzyme activity was determined. The K_m and K_i values represent the averages of two separate experiments.

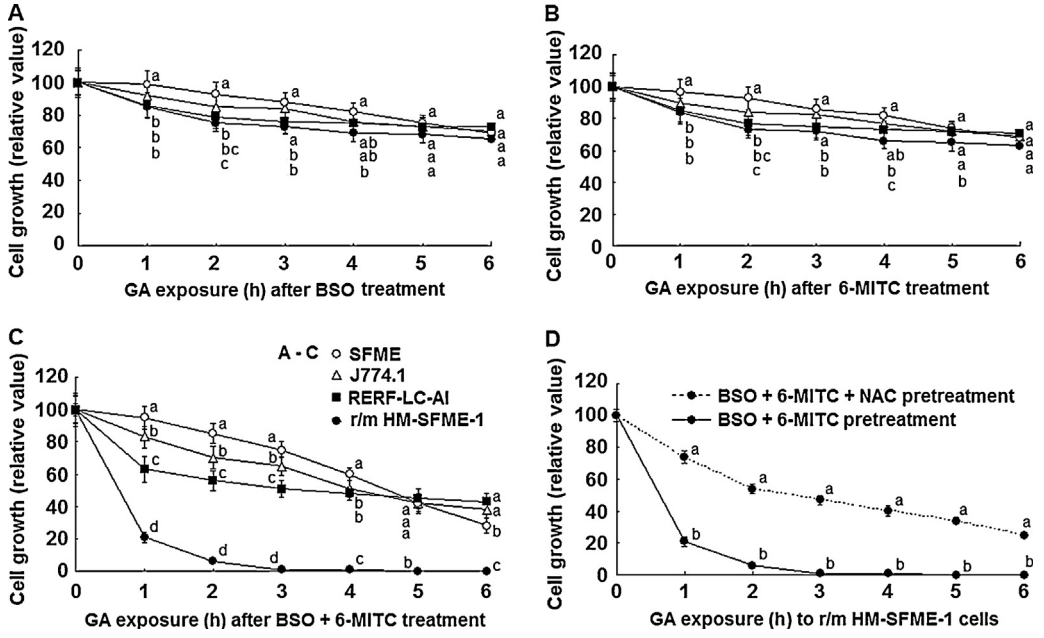

Fig. 7. Antitumor effects of treatment with BSO and/or 6-MITC, followed by GA exposure, on tumor cells. Normal cells and tumor cells were treated with BSO and/or 6-MITC for 4 h to downregulate cellular GSH, followed by exposure to 5 μM GA, a potent antitumor compound [33]. (A) All of the tested cells are affected by the combined treatment with BSO and GA, but the differences between the cell types are not very considerable. (B) Exposure of the cells to GA after the 4 h 6-MITC treatment also does not show great differences between the cell types. (C) Obvious cytotoxicity of GA is observed at an earlier time point (1 h) in the tumor cells (J774.1, RERF-LC-AI, and *r*/*m* HM-SFME-1) compared with the normal SFME cells. GA has significant effects on the tumorigenic *r*/*m* HM-SFME-1 cells, eradicating them in 3 h, while it affects only about 20% of the normal SFME cells. It should be noted that single GA treatment required about 96 h to eradicate the tumor cells in a previous study [33]. (D) The effects of GA on the 6-MITC plus BSO-pretreated *r*/*m* HM-SFME-1 cells are attenuated by addition of 500 μM NAC. The data represent means ± SD of three experiments. Different letters for the treatments indicate significant differences by the Tukey–Kramer test ($P < 0.05$).

studies of GCL. In the present study, Cys-249 in human GCL formed hydrogen bonds with the β-carbon in the cysteinyl moiety of GSH. In *Saccharomyces cerevisiae* GCL, mutation of the equivalent residue, Cys-266, to Ser or Ala doubled its K_m for glutamate and K_i for GSH [48]. In *Trypanosoma brucei* GCL, mutation of Arg-366 (Arg-296 in human GCL) to Ala increased its K_d for glutamate by >160-fold, and mutation of Arg-491 (Arg-427 in human GCL) decreased its enzymatic activity by 70-fold [66], suggesting direct roles in catalysis. Our additional *in silico* analyses of the 6-MITC-GCLC and GSH-GCLC complexes revealed that 6-MITC could override the feedback inhibition of GCL enzyme activity by GSH, by interfering with the hydrogen bonds of the cysteinyl and glutamyl moieties of GSH with Cys-249 and Gln-251, respectively, in the LBS of GCLC. Furthermore, the slight recovery of GCL enzyme activity by 6-MITC in the presence of GSH confirmed the possible overriding effect of 6-MITC on the GSH-induced feedback inhibition, although it was likely to have very minor or no effects owing to the very weak binding of 6-MITC to GCL. To the best of our knowledge, this is the first *in silico* report to propose a possible overriding effect of 6-MITC on the GSH-induced feedback inhibition of GCL enzyme activity. However, the issue of whether or not 6-MITC binds to or inhibits GCL requires further detailed investigations *in vitro*.

The *in vitro* results for the inhibitory effects of the 4 h exposure to 6-MITC on cellular GSH in tumor cells, without inhibition of cell growth in normal cells, showed that 6-MITC can be used for GSH downregulation in tumor cells with minimal damage to normal cells. However, the results for the 24 h exposure to 6-MITC showed that this compound further upregulated cellular GSH after the 4 h exposure in all cell types, even exceeding the control values by 12 h, suggesting that 6-MITC cannot be used as a monotherapy, but can be used for other applications, such as combination therapies. In fact, 6-MITC combined with BSO almost completely depleted GSH in 4 h in the tumorigenic *r*/*m* HM-SFME-1 cells, without depleting GSH in the normal SFME cells. Furthermore, our analysis of the inhibitory effects on GCL enzyme activity showed that the combined treatment significantly affected the enzyme activity compared with the single 6-MITC treatment, although this result could largely arise through the inhibitory effects of BSO.

For any antitumor chemotherapy, an ideal treatment should only affect malignant cells and have minimal cytotoxicity toward normal cells. It is also important that the time required for treatment is as short as possible. In the present study, the 4 h exposure to BSO plus 6-MITC proved to be an effective treatment for GSH depletion. Moreover, with the intensive need for the development of safer agents for chemotherapy, natural products from plants have been expected to be used [67]. We previously reported that the naturally occurring triterpenoid GA from licorice was not only selectively cytotoxic toward tumor cells, but also more potent than some clinically available antitumor agents, such as adriamycin, cisplatin, cytarabine, etoposide, fluorouracil, and manumycin A, in its selectivity [68]. With due consideration of these results, we designed an antitumor strategy for treating normal cells and tumor cells with BSO plus 6-MITC for 4 h followed by GA exposure in the present study. This strategy, which caused GSH depletion in the tumor cells followed by their exposure to a potent antitumor agent, eradicated the tumorigenic *r*/*m* HM-SFME-1 cells in 3 h with minimal damage to the normal SFME cells. Our previous study showed that single GA treatment required about 96 h to eradicate the tumor cells [33]. These observations suggest that our present strategy for depleting GSH in tumor cells using a combined treatment with 6-MITC and eradicating the tumor cells with a naturally occurring antitumor agent, such as GA, could be of great use to impair certain types of tumor cells, such as *r*/*m* HM-SFME-1 cells, that can be chemosensitized by GSH depletion.

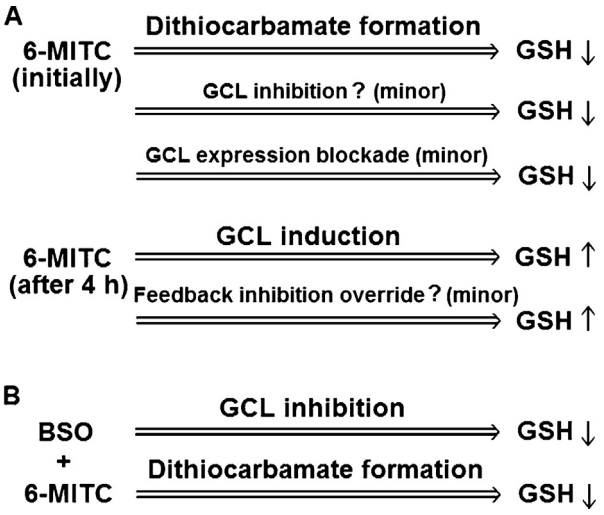

Fig. 8. Proposed mechanism underlying the cellular GSH regulation by 6-MITC. (A) Single 6-MITC treatment initially downregulates cellular GSH, which occurs through the well-established dithiocarbamate formation between 6-MITC and GSH [69,70]. The weak inhibition of the GCL enzyme activity by 6-MITC might be partly responsible for the GSH downregulation. Blockade of GCL by the inhibitory effects of 6-MITC on c-Jun phosphorylation may also be responsible for the GSH downregulation. However, these inhibitory effects are rather weak because the existing cellular GSH is far more abundant [19] than the GSH being synthesized in a few hours. The cellular GSH starts to increase with 6-MITC treatment after 4 h owing to the well-known GCL induction [71] and the possible overriding effect on the GSH-induced feedback inhibition of GCL. (B) The combination treatment downregulates cellular GSH, owing to GCL inhibition by BSO and dithiocarbamate formation by 6-MITC [69,70].

Fig. 8 shows the proposed mechanism underlying the cellular GSH regulation by 6-MITC. The present results showed that single 6-MITC treatment initially downregulated cellular GSH (Fig. 4A–D), which occurred by the well-established dithiocarbamate formation between 6-MITC and GSH [69,70]. The possible weak inhibition of the GCL enzyme activity by 6-MITC (Fig. 6) may be partly responsible for the GSH downregulation. GCLC, the catalytic subunit of GCL, can be induced by Jun N-terminal kinase (JNK)/activating protein 1 (AP-1) signaling [71], and 6-MITC has been reported to inhibit phosphorylation of c-Jun [72]. These observations suggest that 6-MITC possibly blocked GCL expression, although its effect on GSH downregulation was probably rather weak because the existing cellular GSH would have been far more abundant [19] than the GSH being synthesized within a few hours. Subsequently, the cellular GSH started to increase with 6-MITC treatment after 4 h (Fig. 4A–D) through the well-known GCL induction (Fig. 4E) [73] and the possible overriding effect on the GSH-induced feedback inhibition of GCL (Fig. 8A). Furthermore, the combined treatment downregulated cellular GSH through GCL inhibition by BSO and dithiocarbamate formation by 6-MITC (Fig. 8B), which clarifies why cellular GSH was further decreased by BSO plus 6-MITC treatment compared with single BSO treatment, although the GCL enzyme activity was slightly more suppressed by the single BSO treatment than by the combined treatment. In the present study, GSH was downregulated not only by the inhibition of the enzyme activity, but also by the dithiocarbamate formation (depriving the tumor cells of GSH through the effects of 6-MITC).

Fig. 9 shows the proposed mechanism underlying the growth inhibition of tumorigenic *r*/*m* HM-SFME-1 cells by the combined BSO plus 6-MITC treatment for 4 h for GSH depletion, followed by the GA treatment for apoptosis induction (Fig. 7C). BSO is a potent inhibitor of GCL and binds to the LBS of GCLC, the catalytic subunit of the rate-limiting enzyme in GSH synthesis [41–43]. 6-MITC may also inhibit the GCL enzyme activity, albeit weakly (Fig. 6A). The consensus binding sites for AP-1 along with nuclear factor κB (NF-

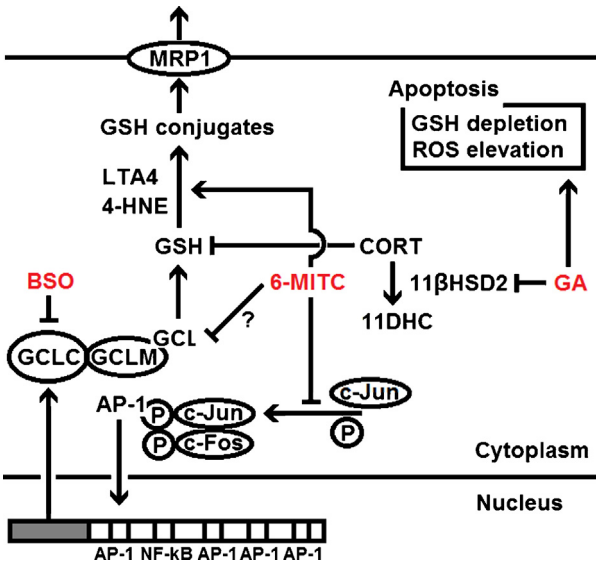

Fig. 9. Proposed mechanism underlying the growth inhibition of tumorigenic *r*/*m* HM-SFME-1 cells by combined BSO plus 6-MITC treatment, followed by GA treatment. BSO is a potent inhibitor of GCL and binds to the LBS of GCLC [41–43]. 6-MITC also inhibits the GCL enzyme activity, albeit weakly (Fig. 6). The consensus binding sites for AP-1 along with NF-κB were identified as the *cis*-acting elements that are largely responsible for the transcriptional regulation of GCLC [71]. 6-MITC blocks the phosphorylation of c-Jun, a critical AP-1 transcription factor [72]. 6-MITC forms dithiocarbamates with GSH [69,70], and endogenous metabolites, such as LTA4 and 4-HNE, also form conjugates with GSH [76]. These GSH conjugates are transported by ABC transporters, such as MRP1 [76]. Taken together, BSO plus 6-MITC treatment significantly downregulates GSH. GA inhibits 11βHSD2 [33] and upregulates CORT, a known downregulator of GSH [77]. GA also elevates the production of ROS in the tumor cells [47], and the depleted GSH by GA treatment together with BSO plus 6-MITC preexposure, which creates a redox imbalance, would lower the antioxidant capacity of the tumor cells and induce apoptosis [33].

κB) were identified as the *cis*-acting elements that are largely responsible for the transcriptional regulation of GCLC [71]. AP-1 transcription factors, such as c-Jun, Jun B, and Jun D, were ascribed to the increased expression of GCLC [74], and c-Jun was reported to be especially critical for the expression of GCLC [75]. 6-MITC blocked the phosphorylation of c-Jun [72], which suggests that the blockade of c-Jun signaling by 6-MITC may be partly responsible for the downregulation of cellular GSH. 6-MITC can form dithiocarbamates with GSH [69,70], and endogenous metabolites, such as leukotriene A4 (LTA4) and 4-hydroxynonenal (4-HNE), also form conjugates with GSH [76]. These GSH conjugates are transported by ATP-binding cassette (ABC) transporters, such as multidrug resistance protein 1 (MRP1) [76], and ABC transporters contribute to the downregulation of GSH. Taken together, the BSO plus 6-MITC treatment significantly downregulated GSH (Figs. 3B and 4A–D). After exposure to BSO plus 6-MITC, the tumor cells were treated with GA. GA inhibited 11β-hydroxysteroid dehydrogenase type 2 (11βHSD2), the enzyme that converts corticosterone (CORT) to 11-dehydrocorticosterone (11DHC) [33]. Consequently, GA upregulated CORT, a known downregulator of GSH [77]. GA also elevated the production of reactive oxygen species (ROS) in the tumor cells [47], and the depleted GSH by GA treatment together with BSO plus 6-MITC pre-exposure, which creates a redox imbalance, would lower the antioxidant capacity of the tumor cells and induce apoptosis [33] in 3 h (Fig. 7C).

In conclusion, we used *in silico* analyses of the ligand–receptor interactions between 6-MITC and GCL for the development of novel antitumor strategies. The results of our *in silico* analyses were confirmed by *in vitro* experimental evidence, and the present study reveals that 6-MITC in combination strategies could be used for depleting GSH and sensitizing tumor cells to antitumor agents, leading to their eradication. GCL and its product GSH have been associated with various cancers and identified as possible targets for the prevention and therapy of cancer [33–45]. Molecular modeling has gained great importance in drug discovery and development [78–80], and further *in silico* analyses of GCL and its interactions with possible ligands are anticipated.

Acknowledgement

This study was partly supported by a Grant-in-Aid from the Promotion and Mutual Aid Corporation for Private Schools of Japan.

References

[1] Kjaer A. Naturally derived isothiocyanates (mustard oils) and their parent glucosides. Fortschr Chem Org Naturst 1960;18:122–76.
[2] Fenwick GR, Heaney RK, Mullin WJ. Glucosinolates and their breakdown products in food and food plants. CRC Crit Rev Food Sci Nutr 1983;18:123–201.
[3] Zhang Y, Talalay P, Cho CG, Posner GH. A major inducer of anticarcinogenic protective enzymes from broccoli: isolation and elucidation of structure. Proc Natl Acad Sci USA 1992;89:2399–403.
[4] Lin JM, Amin A, Trushin N, Hecht SS. Effects of isothiocyanates on tumorigenesis by benzo[a]pyrene in murine tumor models. Cancer Lett 1993;74:151–9.
[5] Zhang Y, Kensler TW, Cho CG, Posner GH, Talalay P. Anticarcinogenic activities of sulforaphane and structurally related synthetic norbornyl isothiocyanates. Proc Natl Acad Sci USA 1994;91:3147–50.
[6] Zhang Y, Talalay P. Anticarcinogenic activities of organic isothiocyanates: chemistry and mechanisms. Cancer Res 1994;54:1976–81.
[7] Fuke Y, Haga Y, Ono H, Nomura T, Ryoyama K. Anti-carcinogenic activity of 6-methylsulfinylhexyl isothiocyanate-, an active anti-proliferative principal of wasabi (Eutrema wasabi Maxim). Cytotechnology 1997;25:197–203.
[8] Yano T, Yajima S, Virgona N, Yano Y, Otani S, Kumagai H, et al. The effect of 6-methylthiohexyl isothiocyanate isolated from *Wasabia japonica* (wasabi) on 4-(methylnitrosamino)-1-(3-pyridyl)-1-buatnone-induced lung tumorigenesis in mice. Cancer Lett 2000;155:115–20.
[9] Prochaska HJ, Santamaria AB, Talalay P. Rapid detection of inducers of enzymes that protect against carcinogens. Proc Natl Acad Sci USA 1992;89:2394–8.
[10] Maheo K, Morel F, Langouet S, Kramer H, Le Ferrec E, Ketterer B, et al. Inhibition of cytochromes P-450 and induction of glutathione S-transferases by sulforaphane in primary human and rat hepatocytes. Cancer Res 1997;57:3649–52.
[11] Hou DX, Fukuda M, Fujii M, Fuke Y. Transcriptional regulation of nicotinamide adenine dinucleotide phosphate: quinone oxidoreductase in murine hepatoma cells by 6-(methylsufinyl)hexyl isothiocyanate, an active principle of wasabi (Eutrema wasabi Maxim). Cancer Lett 2000;161:195–200.
[12] Hou DX, Fukuda M, Fujii M, Fuke Y. Induction of NADPH: quinone oxidoreductase in murine hepatoma cells by methylsulfinyl isothiocyanates: methyl chain length-activity study. Int J Mol Med 2000;6:441–4.
[13] Nakamura Y, Ohigashi H, Masuda S, Murakami A, Morimitsu Y, Kawamoto Y, et al. Redox regulation of glutathione S-transferase induction by benzyl isothiocyanate: correlation of enzyme induction with the formation of reactive oxygen intermediates. Cancer Res 2000;60:219–25.
[14] Singletary K, MacDonald C. Inhibition of benzo[a]pyrene- and 1,6-dinitropyrene-DNA adduct formation in human mammary epithelial cells bydibenzoylmethane and sulforaphane. Cancer Lett 2000;155:47–54.
[15] Ryoyama K, Mori N, Nara M, Kidachi Y, Yamaguchi H, Fuke Y. Augmented gene expression of quinone reductase by 6-(methylsulfinyl)hexyl isothiocyanate through avoiding its cytotoxicity. Anticancer Res 2003;23:3741–8.
[16] Nomura T, Shinoda S, Yamori T, Sawaki S, Nagata I, Ryoyama K, et al. Selective sensitivity to wasabi-derived 6-(methylsulfinyl)hexyl isothiocyanate of human breast cancer and melanoma cell lines studied in vitro. Cancer Detect Prev 2005;29:155–60.
[17] Fuke Y, Shinoda S, Nagata I, Sawaki S, Murata M, Ryoyama K, et al. Preventive effect of oral administration of 6-(methylsulfinyl)hexyl isothiocyanate derived from wasabi (*Wasabia japonica* Matsum) against pulmonary metastasis of B16-BL6 mouse melanoma cells. Cancer Detect Prev 2006;30:174–9.
[18] Noshita T, Kidachi Y, Funayama S, Kiyota H, Yamaguchi H, Ryoyama K. Anti-nitric oxide production activity of isothiocyanates correlates with their polar surface area rather than their lipophilicity. Eur J Med Chem 2009;44:4931–6.
[19] Meister A, Anderson ME. Glutathione. Annu Rev Biochem 1983;52:711–60.
[20] Meister A. In: Dolphin D, Avramovich A, Poulson R, editors. Metabolism and function of glutathione (Glutathione. Chemical, biochemical and medical aspects, Part A). New York: John Wiley & Sons, Inc; 1989. p. 367–474.
[21] Kosower NS, Kosower EM. The glutathione status of cells. Int Rev Cytol 1978;54:109–60.
[22] Meister A. Glutathione deficiency produced by inhibition of its synthesis, and its reversal; applications in research and therapy. Pharmacol Ther 1991;51:155–94.
[23] Hall AG. The role of glutathione in the regulation of apoptosis. Eur J Clin Invest 1999;29:238–45.
[24] Manna SK, Kuo MT, Aggarwal BB. Overexpression of gamma-glutamylcysteine synthetase suppresses tumor necrosis factor-induced apoptosis and activation

of nuclear transcription factor-kappa B and activator protein-1. Oncogene 1999;18:4371–82.
[25] Botta D, Franklin CC, White CC, Krejsa CM, Dabrowski MJ, Pierce RH, et al. Glutamate-cysteine ligase attenuates TNF-induced mitochondrial injury and apoptosis. Free Radic Biol Med 2004;37:632–42.
[26] Orlowski M, Meister A. Partial reactions catalyzed by -glutamylcysteine synthetase and evidence for an activated glutamate intermediate. J Biol Chem 1971;246:7095–105.
[27] Griffith OW, Mulcahy RT. The enzymes of glutathione synthesis: gamma-glutamylcysteine synthetase. Adv Enzymol Relat Areas Mol Biol 1999;73: 209–67.
[28] Strumeyer DH, Bloch K. Some properties of gamma-glutamylcysteine synthetase. J Biol Chem 1960;235:PC27.
[29] Yip B, Rudolph FB. The kinetic mechanism of rat kidney gamma-glutamylcysteine synthetase. J Biol Chem 1976;251:3563–8.
[30] Sierra-Rivera E, Dasouki M, Summar ML, Krishnamani MRS, Meredith M, Rao PN, et al. Assignment of the human gene (GLCLR) that encodes the regulatory subunit of gamma-glutamylcysteine synthetase to chromosome 1p21. Cytogenet Cell Genet 1996;72:252–4.
[31] Walsh AC, Li W, Rosen DR, Lawrence DA. Genetic mapping of GLCLC, the human gene encoding the catalytic subunit of gamma-glutamyl-cysteine synthetase, to chromosome band 6p12 and characterization of a polymorphic trinucleotide repeat within its 5′ untranslated region. Cytogenet Cell Genet 1996;75:14–6.
[32] Wild AC, Mulcahy RT. Regulation of gamma-glutamylcysteine synthetase subunit gene expression: insights into transcriptional control of antioxidant defenses. Free Radic Res 2000;32:281–301.
[33] Yamaguchi H, Yu T, Noshita T, Kidachi Y, Kamiie K, Yoshida K, et al. Ligand–receptor interaction between triterpenoids and the 11beta-hydroxysteroid dehydrogenase type 2 (11betaHSD2) enzyme predicts their toxic effects against tumorigenic r/m HM-SFME-1 cells. J Biol Chem 2011;286:36888–97.
[34] Godwin AK, Meister A, O'Dwyer PJ, Huang CS, Hamilton TC, Anderson ME. High resistance to cisplatin in human ovarian cancer cell lines is associated with marked increase of glutathione synthesis. Proc Natl Acad Sci USA 1992;89:3070–4.
[35] Mulcahy RT, Bailey HH, Gipp JJ. Up-regulation of gamma-glutamylcysteine synthetase activity in melphalan-resistant human multiple myeloma cells expressing increased glutathione levels. Cancer Chemother Pharmacol 1994;34:67–71.
[36] Mulcahy RT, Bailey HH, Gipp JJ. Transfection of complementary DNAs for the heavy and light subunits of human gamma-glutamylcysteine synthetase results in an elevation of intracellular glutathione and resistance to melphalan. Cancer Res 1995;55:4771–5.
[37] Griffith OW, Friedman HS. In: Chou TC, Rideout DC, editors. Glutathione and resistance to anticancer therapies (Synergism and antagonism in chemotherapy). San Diego: Academic Press; 1991. p. 245–85.
[38] Lewandowicz GM, Britt P, Elgie AW, Williamson CJ, Coley HM, Hall AG, et al. Cellular glutathione content, in vitro chemoresponse, and the effect of BSO modulation in samples derived from patients with advanced ovarian cancer. Gynecol Oncol 2002;85:298–304.
[39] Ramanathan B, Jan KY, Chen CH, Hour TC, Yu HJ, Pu YS. Resistance to paclitaxel is proportional to cellular total antioxidant capacity. Cancer Res 2005;65:8455–60.
[40] Yoshida A, Takemura H, Inoue H, Miyashita T, Ueda T. Inhibition of glutathione synthesis overcomes Bcl-2-mediated topoisomerase inhibitor resistance and induces nonapoptotic cell death via mitochondrial-independent pathway. Cancer Res 2006;66:5772–80.
[41] Griffith OW. Mechanism of action, metabolism, and toxicity of buthionine sulfoximine and its higher homologs, potent inhibitors of glutathione synthesis. J Biol Chem 1982;257:13704–12.
[42] O'Dwyer PJ, Hamilton TC, LaCreta FP, Gallo JM, Kilpatrick D, Halbherr T, et al. Phase I trial of buthionine sulfoximine in combination with melphalan in patients with cancer. J Clin Oncol 1996;14:249–56.
[43] Chen X, Carystinos GD, Batist G. Potential for selective modulation of glutathione in cancer chemotherapy. Chem Biol Interact 1998;112:263–75.
[44] Tokutake N, Hiratake J, Katoh M, Irie T, Kato H, Oda JI. Design, synthesis and evaluation of transition-state analogue inhibitors of *Escherichia coli* gamma-glutamylcysteine synthetase. Bioorg Med Chem 1998;6:1935–53.
[45] Hiratake J, Irie T, Tokutake N, Oda JI. Recognition of a cysteine substrate by *E. coli* gamma-glutamylcysteine synthetase probed by sulfoximine-based transition-state analogue inhibitors. Biosci Biotechnol Biochem 2002;66:1500–14.
[46] Yamaguchi H, Akitaya T, Kidachi Y, Kamiie K, Umetsu H. Homology modeling and structural analysis of human γ-glutamylcysteine ligase catalytic subunit for antitumor drug development. J Biophys Chem 2012;3:238–48.
[47] Yamaguchi H, Yu T, Kidachi Y, Noshita T, Kamiie K, Akitaya T, et al. Selective toxicity of glycyrrhetinic acid against tumorigenic r/m HM-SFME-1 cells is potentially attributed to downregulation of glutathione. Biochimie 2011;93: 1172–8.
[48] Biterova EI, Barycki JJ. Structural basis for feedback and pharmacological inhibition of *Saccharomyces cerevisiae* glutamate cysteine ligase. J Biol Chem 2010;285:14459–66.
[49] Levitt M. Accurate modeling of protein conformation by automatic segment matching. J Mol Biol 1992;226:507–33.
[50] Fechteler T, Dengler U, Schomberg D. Prediction of protein three-dimensional structures in insertion and deletion regions: a procedure for searching databases of representative protein fragments using geometric scoring criteria. J Mol Biol 1995;253:114–31.
[51] Goto J, Kataoka R, Muta H, Hirayama N. ASEDock-docking based on alpha spheres and excluded volumes. J Chem Inf Model 2008;48:583–90.
[52] Hirakawa H, Akita H, Fujiwara T, Sugai M, Kuhara S. Structural insight into the binding mode between the targeting domain of ALE-1 (92AA) and pentaglycine of peptidoglycan. Protein Eng Des Sel 2009;22:385–91.
[53] Halgren TA. Merck molecular force field. I. Basis, form, scope, parameterization, and performance of MMFF94. J Comput Chem 1996;17:490–519.
[54] Nomura T, Matano S, Okada G, Tokuyama H, Hori I, Nakamura S, et al. Establishment of a metastatic murine cell line carrying the human C-Ha-ras. In Vitro Cell Dev Biol Anim 1993;29A:614–6.
[55] Carmichael J, DeGraff WG, Gazdar AF, Minna JD, Mitchell JB. Evaluation of a tetrazolium-based semiautomated colorimetric assay: assessment of radiosensitivity. Cancer Res 1987;47:943–6.
[56] Huang CS, Chang LS, Anderson ME, Meister A. Catalytic and regulatory properties of the heavy subunit of rat kidney gamma-glutamylcysteine synthetase. J Biol Chem 1993;268:19675–80.
[57] Biterova EI, Barycki JJ. Mechanistic details of glutathione biosynthesis revealed by crystal structures of *Saccharomyces cerevisiae* glutamate cysteine ligase. J Biol Chem 2009;284:32700–08.
[58] Labute P. The generalized Born/volume integral implicit solvent model: estimation of the free energy of hydration using London dispersion instead of atomic surface area. J Comput Chem 2008;29:1693–8.
[59] Couzin J. Cancer drugs. Smart weapons prove tough to design. Science 2002;298:522–5.
[60] Frantz S. Drug discovery: playing dirty. Nature 2005;437:942–3.
[61] Trachootham D, Zhou Y, Zhang H, Demizu Y, Chen Z, Pelicano H, et al. Selective killing of oncogenically transformed cells through a ROS-mediated mechanism by beta-phenylethyl isothiocyanate. Cancer Cell 2006;10:241–52.
[62] Rappa G, Gamcsik MP, Mitina RL, Baum C, Fodstad O, Lorico A. Retroviral transfer of MRP1 and gamma-glutamyl cysteine synthetase modulates cell sensitivity to L-buthionine-S,R-sulphoximine (BSO): newrationale for the use of BSO in cancer therapy. Eur J Cancer 2003;39:120–8.
[63] Akan I, Akan S, Akca H, Savas B, Ozben T. Multidrug resistance-associated protein 1 (MRP1) mediated vincristine resistance: effects of N-acetyl-cysteine and buthionine sulfoximine. Cancer Cell Int 2005;5:22.
[64] Anderson CP, Tsai JM, Meek WE, Liu RM, Tang Y, Forman HJ, et al. Depletion of glutathione by buthionine sulfoxine is cytotoxic for human neuroblastoma cell lines via apoptosis. Exp Cell Res 1999;246:183–92.
[65] Friesen C, Kiess Y, Debatin KM. A critical role of glutathione in determining apoptosis sensitivity and resistance in leukemia cells. Cell Death Differ 2004;11(Suppl. 1):S73–85.
[66] Abbott JJ, Ford JL, Phillips MA. Substrate binding determinants of *Trypanosoma brucei* gamma-glutamylcysteine synthetase. Biochemistry 2002;41: 2741–50.
[67] Martin R, Carvalho J, Ibeas E, Hernandez M, Ruiz-Gutierrez V, Niet ML. Acidic triterpenes compromise growth and survival of astrocytoma cell lines by regulating reactive oxygen species accumulation. Cancer Res 2007;67: 3741–51.
[68] Yu T, Yamaguchi H, Noshita T, Kidachi Y, Umetsu H, Ryoyama K. Selective cytotoxicity of glycyrrhetinic acid against tumorigenic r/m HM-SFME-1 cells: potential involvement of H-Ras downregulation. Toxicol Lett 2010;192: 425–30.
[69] Kolm RH, Danielson UH, Zhang Y, Talalay P, Mannnervik B. Isothiocyanates as substrates for human glutathione transferases: structure-activity studies. Biochem J 1995;311:453–9.
[70] Cacciatore I, Cornacchia C, Pinnen F, Mollica A, Di Stefano A. Prodrug approach for increasing cellular glutathione levels. Molecules 2010;15:1242–64.
[71] Yang H, Wang J, Huang Z, Ou X, Lu SC. Cloning and characterization of the 5′-flanking region of the rat glutamate-cysteine ligase catalytic subunit. Biochem J 2001;357:447–55.
[72] Uto T, Fujii M, Hou DX. Effects of 6-(methylsulfinyl)hexyl isothiocyanate on cyclooxygenase-2 expression induced by lipopolysaccharide, interferon-γ and 12-*O*-tetradecanoylphorbol-13-acetate. Oncol Rep 2007;17:233–8.
[73] Emmert SW, Desai D, Amin S, Richie J.P. Jr. Enhanced Nrf2-dependent induction of glutathione in mouse embryonic fibroblasts by isoselenocyanate analog of sulforaphane. Bioorg Med Chem Lett 2010;20:2675–9.
[74] Sekhar KR, Meredith MJ, Kerr LD, Soltaninassab SR, Spitz DR, Xu ZQ, et al. Expression of glutathione and c-glutamylcysteine synthetase mRNA is Jun dependent. Biochem Biophys Res Commun 1997;234:588–93.
[75] Dickinson DA, Iles KE, Watanabe N, Iwamoto T, Zhang H, Krzywanski DM, et al. 4 hydroxynonenal induces glutamate cysteine ligase through JNK in HBE1 cells. Free Radic Biol Med 2002;33:974–87.
[76] Cole SPC, Deeley RG. Transport of glutathione and glutathione conjugates by MRP1. Trends Pharmacol Sci 2006;27:438–46.
[77] Zafir A, Banu N. Modulation of in vivo oxidative status by exogenous corticosterone and restraint stress in rats. Stress 2009;12:167–77.
[78] Kurogi Y, Guner OF. Pharmacophore modeling and three-dimensional database searching for drug design using catalyst. Curr Med Chem 2001;8: 1035–55.
[79] Ekins S. Predicting undesirable drug interactions with promiscuous proteins in silico. Drug Discovery Today 2004;9:276–85.
[80] Jorgensen WL. The many roles of computation in drug discovery. Science 2004;303:1813–8.